TECHNIUM

Technium Vol. 2, Issue 7 pp.64-76 (2020)
ISSN: 2668-778X
www.techniumscience.com

Management of Hybrid Renewable Energy Systems Using Differential Hybrid Petri Nets

Kennedy FOHOUE-TCHENDJOU [1,2,3] Vivient Corneille KAMLA[2], Daniel TIEUDJO[2] and Laurent BITJOKA[1]

[1] Laboratory of Energy, Signal, Imagery and Automatics (LESIA),Cameroon
[2] Laboratory of Experimental Mathematics (LAMEX),Cameroon

E-mail: kennedyfohoue@gmail.com

Abstract. Investigations in this paper concern management of Hybrid Renewable Energy systems (HREs). To achieve it, a supervisory system based on hybrid systems concept is designed, in order to ensure power flow between energy generators (solar panel and pico-hydroelectric), batteries and load. Differential Hybrid Petri Net is used to model the proposed supervisory and simulations are made in Matlab environment. Results obtained present a good performance criteria Loss of Power Supply Probability, and this show the effectiveness of our approach in the coordination of HREs components during the energy sharing process by reducing load shedding in microgrid system.
Keyword: Differential Hybrid Petri Net, management, Hybrid Renewable Energy, Loss of Power Supply Probability

1. Introduction

Supervision of a power electric generation is an essential challenge for many hybrid energy systems. The systems which are built on renewable sources represent an opportunity to the power balance of a country, particular in rural areas for supply electricity. Indeed, it is estimated that 18% of the global population do not have access to electrical energy [1]. Among the multiple reasons of this low penetration of electricity in remote areas, we have the obsolescence of the main grids, rural population which are located in rugged terrain areas and low exploitation of available renewable energy sources. That is why, the development of decentralised stand-alone Hybrid Renewable Energy Systems represents an important alternative this last decade for economic, sociological, and ecological factors. In fact, implantation of such systems in most of the cases does not require enormous financial means and low cost maintenances; moreover , it allows the rural populations to directly has an electricity supply and due to the

[3] Present address: Department of Electrical Engineering, Energetic and Automatic, P.O. Box 455, The University of Ngaoundere.

scale of the installation, damages on environment are significantly reduced. Among the renewable sources of energy, the utilisation of solar and wind power have become increasingly important, attractive, and cost effective [2]. However, the choice of a suitable configuration of hybrid installation for a given site depends on many factors, including the load power, geography site, the topographical features and climate conditions of the region [3]. Thus, to consider reasons mentioned by E.M.Nfah [4], Kenfack [5] and Abanda in [6], the decentralised HREs is composed of photovoltaic/pico hydroelectric turbine and battery energy storage systems. Moreover, these components are interconnected on DC bus via power converters. Electrical energy generated by such system is submitted to many disturbances which are caused by the random behaviour of weather conditions, and sometimes unpredictable profile of the load. These fluctuations are caused by several dysfunctions at DC bus microgrid like peaks and drop of power, outages of current and bad quality of energy (unstable voltage and frequency). To remedy these problems, some installations are equipped with some conventional generators which use fossil fuel [7], in order to guarantee availability of power. Unfortunately, these generators have negative impacts on environment such as air pollution and climate change [8]. Therefore, to follow these systems, we need a sophisticated methods to control the energy generation. Several researches have concerned with supervisory of hybrid power sources according to the availability of the renewable energy sources, using the graphical tools of modelling. Indeed, those works are based on the modelling of continuous events of a system with bond graphs, energetic macroscopic representation and causal ordering graph [9], other focused only on discrete events by using Petri Nets [10], [11], [12] and automata [13]. In this framework, HREs is considered as a hybrid system with continuous and discrete events. Due to this fact, Hybrid Automata [14] and Differential Hybrid Petri Nets (DHPN) [15] are able to model both events. We use DHPN, because it can allow the representation of conflicts, casualties, resource sharing and synchronisation [16]; this is not the case with Hybrid Automata. DHPN have been recently introduced to model and simulate hybrid power systems [15] and [17]. In Sousa [15] hybrid electrical energy systems are modelled and analysed like a hybrid system through the formalism of Differential Hybrid Petri Nets (DHPN). In comparison with this last work, we focus on the control of decentralised stand-alone HREs, but the difference is based on the topology and design of different operational modes of the system. Simulation is implemented to prove effectiveness of our approach on the proposed management strategy. The following assumptions are made: we suppose that the voltage on the direct current bus is quite stable and the photovoltaic generator is working on his maximum point power.

The paper has the following organisation: Section 2 presents the configuration of the HRE system, then in Section 3 we discuss the mathematical modelling of each component of the HRE system. After this, designing of the supervisory control of the stand-alone hybrid generation electrical system and definition of the Differential Hybrid Petri Nets formalism are shown in Section 4. Section 5 is focused on the modelling of supervisory control by DHPN tool, the validation of the model by simulation and the discussion of the results are done in Section 6, Section 7 sums-up the conclusion.

Technium Vol. 2, Issue 7 pp.64-76 (2020)
ISSN: 2668-778X
www.techniumscience.com

2. Topology of the decentralised stand-alone Hybrid Renewable Energy Systems (HREs)

Hybrid Renewable Energy System is a system which has at least two renewable sources of energy. This appears to be one of the most attractive solutions to overcome the lack of electricity and environmental problems. Cameroon has a high hydro potential estimated to $294TWh/year$ [6], and the rivers of rural areas are fed by two main catchments from the Adamawa high plateau and the western highlands. Which allows these rivers to have for example, a mean discharge flow of $7m^3/s$ in Far North region [18]. Furthermore, estimates of 5.8 and $4kWh/day/m^2$ respectively in the Northern and Southern regions of the country of global solar radiation[6], solar energy is abundantly distributed all round the year especially in the dry season which usually runs from November to March every year. Even in the rainy season the solar resource is always richly available [16]. Due to these assets, HRES describes in Figure 1 is composed of heterogeneous renewable sources (solar panel and pico-hydroelectric). We also have a storage system which is made by battery banks, and power electronic converter (Zero Voltage Switching). All these components are coupled on a DC bus.

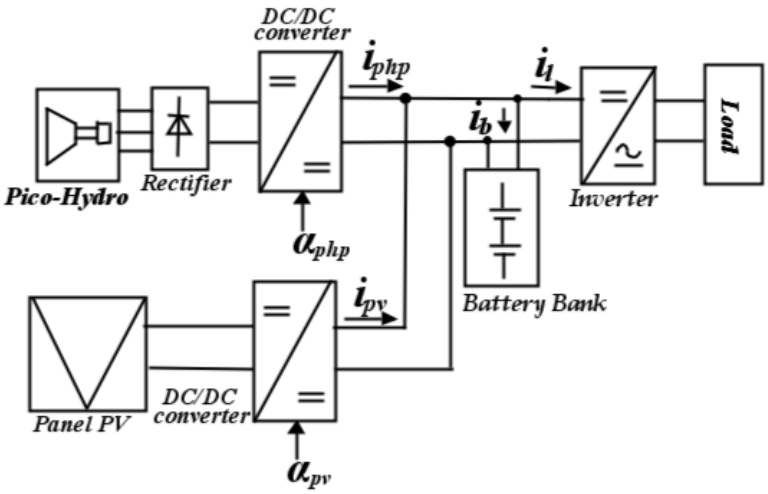

Figure 1: Topology of Stand-alone HRES

3. Mathematical Modelling of a Decentralised Stand-alone HRES

The mathematical model for each component of the topology is presented. A proper derivation of mathematical model for the system is necessary to have a better analysis of the system dynamics in transient and steady-state operation.

3.1. Pico-hydro power plant

Power plant used is for the smallest scale with capacity less than $5Kw$ [4]. The dynamic model of generators is based on the reference Park (d-q) with orientation of the stator flux. It permits to separate the representations on d and q axes. In this case

we consider only the vector control method by orientation of the stator flux. The field is then rotated and oriented according to the stator flux of direct axes. It follows that

$$\Phi_{sq} = \Phi_s; \Phi_{sd} = 0 \tag{1}$$

Moreover we neglect stator resistance and we are on steady state; the stator voltage is given by:

$$\begin{cases} v_{sd} = & R_s i_{sd} + \frac{d\Phi_{sd}}{dt} \simeq 0 \\ v_{sq} = & R_s i_{sq} + \omega_s \Phi_{sd} \simeq v_s = \omega_s \Phi_s \end{cases} \tag{2}$$

And the rotor voltage is given by

$$\begin{cases} v_{rd} = & R_r i_{rd} + \sigma L_r \frac{di_{rd}}{dt} + \sigma L_r \omega_r i_{rq} \\ v_{rq} = & R_r i_{rq} + \sigma L_r \frac{di_{rq}}{dt} - \sigma L_r \omega_r i_{rd} + \omega_r \frac{Lm}{Ls} \Phi_s \end{cases} \tag{3}$$

Thus, by combining the voltage and mechanical torque equation of the whole pico-hydro power plant system, we obtain:

$$\begin{cases} \frac{di_{rd}}{dt} = & -\frac{R_r}{\sigma L_r} i_{rd} - \omega_r i_{rq} - \frac{1}{\sigma L_r} v_{rd} \\ \frac{di_{rq}}{dt} = & -\frac{R_r}{\sigma L_r} i_{rq} + \omega_r i_{rd} - \omega_r \frac{L_m}{\sigma L_r L_s} \Phi_s + \frac{1}{\sigma L_r} v_{rq} \\ \frac{d\Omega_a}{dt} = & \frac{1}{J} \left(T_{tub} - T_{em} - f_v \Omega_a \right) \end{cases} \tag{4}$$

with $T_{turb} = \eta_t \frac{\rho g h Q(t)}{\Omega_a}$and $T_{em} = -p\Phi_s \frac{L_m}{L_s} i_{rq}$
or we have $\omega_r = \omega_s - p\Omega_a = g\omega_s$; $v_{rd} = 0$ and $v_{rq} = 0$. This leads to the following system:

$$\begin{cases} \frac{di_{rd}}{dt} = & -\frac{R_r}{\sigma L_r} i_{rd} - (\omega_s - p\Omega_a) i_{rq} \\ \frac{di_{rq}}{dt} = & +(\omega_s - p\Omega_a) i_{rd} - \frac{R_r}{\sigma L_r} i_{rq} - (\omega_s - p\Omega_a) \frac{L_m \Phi_s}{\sigma L_r L_s} \\ \frac{d\Omega_a}{dt} = & k_v \frac{Q}{\Omega_a} + \frac{pL_m \Phi_s}{JL_s} i_{rq} - \frac{f_v}{J} \Omega_a \end{cases} \tag{5}$$

This system can be written as

$$\frac{d}{dt} \begin{bmatrix} i_{rd} \\ i_{rq} \\ \Omega_a \end{bmatrix} = \begin{bmatrix} \frac{-R_r}{L_r \sigma} & -\omega_s & 0 \\ \omega_s & \frac{-R_r}{L_r \sigma} & \frac{pL_m \Phi_s}{\sigma L_s L_r} \\ 0 & \frac{pL_m \Phi_s}{JL_s} & -\frac{f_v}{J} \end{bmatrix} \begin{bmatrix} i_{rd} \\ i_{rq} \\ \Omega_a \end{bmatrix} + \begin{bmatrix} p\Omega_a i_{rq} \\ -p\Omega_a i_{rd} - \frac{\omega_s L_m \Phi_s}{\sigma L_s L_r} \\ k_v \frac{Q}{\Omega_a} \end{bmatrix} \tag{6}$$

where $k_v = \eta_t \rho g h / J$
Thus, the active and reactive power produced is given by the following relations:

$$\begin{cases} P_s = -v_s \frac{L_m}{L_s} i_{qr} \\ Q_s = v_s \frac{\Phi_s}{L_s} - v_s \frac{L_m}{L_s} i_{dr} \end{cases} \tag{7}$$

3.2. The photovoltaic generator

We suppose that the system is working at his maximum power point tracking. Mathematical model of the output current is given by the Equation (8) see [19].

$$i_{pv} = I_{ph} - I_D - I_p \tag{8}$$

Where I_{ph} the photo-generated current depends on both irradiance and cell temperature expressed as:

$$I_{ph} = \frac{G}{G_{ref}}[I_{cc,ref} + K_i(T_c - T_{c,ref})] \tag{9}$$

The diode current I_D is given by:

$$I_D = I_{sat}[exp(\frac{V_{pv} + R_s I_{pv}}{\eta V_t}) - 1] \tag{10}$$

where $q = 1.602 \times 10^{-19} C$ Electron charge and $k = 1.381 \times 10^{-23} JK^{-1}$ is the Boltzmann constant; the reverse saturation current is given by:

$$I_{sat} = A * exp\left[\frac{qE_g}{\eta k}\left(\frac{1}{T_{c,ref}} - \frac{1}{T_c}\right)\right] \tag{11}$$

where

$$A = I_{sat,ref}\left(\frac{T_c}{T_{c,ref}}\right)^3 \tag{12}$$

Taking into account that the shunt resistance R_p is usually very large: $(R_p \to \infty \Rightarrow I_p = 0)$, the current produced by the photovoltaic generator is given by

$$i_{pv} = N_p I_{ph} - N_p I_{sat}[exp(\frac{v_{pv} + R_s I_{pv}}{\eta V_t N_{sc} N_p}) - 1] \tag{13}$$

and finally, the power supplied by the photovoltaic plant converter is given by:

$$P_{pv} = v_{pv} i_{pv} \tag{14}$$

3.3. Battery bank

Although it is an additional source of energy for the system, the battery bank also constitutes a load for the grid. His function is to store the electric power generated by both plants PV and Pico-hydroelectric, in order to be used when there is a deficit of energy produced by the main generators. The expression of the battery current of the system can be modelled by equation (15) (see [20]).

$$i_{bat} = i_{php} + i_{pv} - i_L \tag{15}$$

The voltage at the terminals of the battery is expressed by:

$$v_b = E_b + v_c + (i_{php} + i_{pv} - i_L)\, R_b \tag{16}$$

with

$$\dot{v}_c = \frac{1}{C_b}\left(i_{php} + i_{pv} - i_L\right) \tag{17}$$

The charge and discharge processes of the battery correspond to:

- Discharge process :

$$V_{BBd} = 1,965 + 0,12SOC(t) - \frac{I_{BB}}{C_{10}} \times K1 \tag{18}$$

where $K1 = \left(\frac{4}{1+|i_{bat}|^{1,3}} + \frac{0,27}{SOC(t)^{1,5}} + 0,02)(1 - 0,007\Delta T\right)$

- Charge process :

$$V_{BBc} = 2 + 0,16SOC(t) - \frac{I_{BB}}{C_{10}} \times K2 \tag{19}$$

with $K2 = \left(\frac{6}{1+|i_{bat}|^{0,86}} + \frac{0,48}{(1-SOC(t))^{1,2}} + 0,036)(1 - 0,0025\Delta T\right)$

I_{BB} denotes the intensity delivered by the battery (A).

Moreover, to follow the level of energy in the battery bank we use the parameter SOC which is evaluated in [15] by the Equation (20).

$$SOC(t) = SOC(0) + \int_0^t \frac{i_{bat}}{C_b} dt \tag{20}$$

4. Supervisory control design

4.1. Grid Connected Stand-alone Generation Hybrid System

The Figure 2 shows the structure of the control adopted particularly the high level control. In fact, it presents the three commands C_1,C_2 and C_3 which are the different contactors of the system, fixed respectively between the generators, load and battery. The capacity to supply electricity by HRES is directly linked to weather conditions. Fundamentally, it is able to manage the power flow between generators and load according to some constraints (environmental and system component). As criteria to define different operating modes, we consider the behaviour of storage system, particularly the State of Charge (SOC) and the energy balance between the total generation (solar + Pico hydroelectric) and the load demand.

Low level control is not part of this study. Nevertheless, functions $C_{I1}(P)$,$C_{I2}(P)$ and $C_s(P)$ are the proportional integral corrector functions respectively of the current and voltages.

4.2. Design of the Control Operating Mode

First we will define the power error P_c:

$$P_c = P_{php} + P_{pv} - P_L \tag{21}$$

According to the values of P_c, we will design a supervisory high level control in order

Technium Vol. 2, Issue 7 pp.64-76 (2020)
ISSN: 2668-778X
www.techniumscience.com

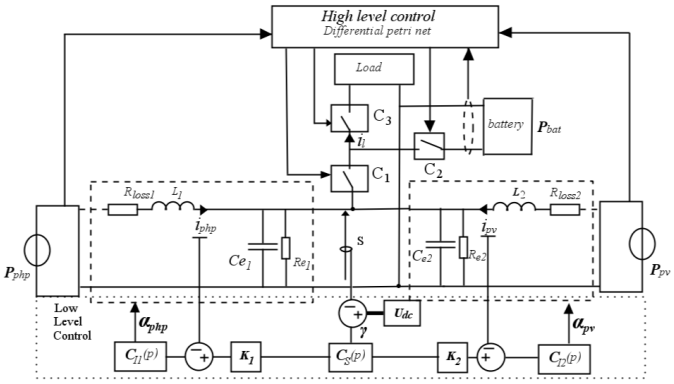

Figure 2: High level Control

to ensure the power supply of consumers. Thus, the commutations between the modes are given according to the different values of the equation 21 and the state of battery value equation 20. The following rules can be formulated :

Mode 1: During this state, available plants power is enough to supply load and the batteries are empties. In this case, load is entirely fed by main generators. Due to the fact that SOC is at the minimum level, batteries are charged by excess energy. In this situation, the generators supplied the consumers alone.

Mode 2: Power flow in this mode is almost in equilibrium, when the both plants PV and Pico-hydro can not supply a power required by the load, battery system is connected , to generate energy enough for the load . Duration of this mode is sustained by the capacity of the battery to stay in $SOC_{min} \leq SOC \leq SOC_{max}$.

Mode 3: The powers from generators and batteries are less than the required power from consumers. It cannot be used to track during a long time load. This phase is sustained until the state of charge surpasses the minimum threshold SOC_{min}. Therefore the consumers are disconnected to allow the full charge of the battery bank.

According to the state of switches, this can be recapitulated in Table 1:

Table 1: Conditions for the selection of operational mode

Mode	**Constrains**	**States of contactors**
1	$P_C \geq 0$ and $SOC \geq SOC_{\max}$	$O_1 = 0; O_2 = 1; O_3 = 1$
2	$P_C \geq 0$ and $SOC_{\min} \leq SOC \leq SOC_{\max}$	$O_1 = 1; O_2 = 1; O_3 = 1$
3	$P_C \leq 0$ and $SOC \leq SOC_{\min}$	$O_1 = 1; O_2 = 1; O_3 = 0$

In this table when $O_i = 0$ it means that the contactor C_i is opened and if $O_i = 1$ the contactor C_i is closed, with $i = \{1, 2, 3\}$. During his exploitation, the discrete events mentioned below are interacted with continuous events which dynamics are modelled by differential equations. Therefore, to represent graphically all these phenomenon we used DHPN which is defined below.

Technium Vol. 2, Issue 7 pp.64-76 (2020)
ISSN: 2668-778X
www.techniumscience.com

4.3. Differential Hybrid Petri Net

Differential Hybrid Petri Net is one of the extension of Petri Net. Initially defined by Demongodin in [21], this formalism has been improved by many researchers. In this work, the following definition is adopted.

Definition 4.1 *A Differential Hybrid Petri Net is defined by* $DHPN = \langle X_{DF}, X_D, T_D, T_{DF}, P_D, P_{DF}, Pre(P_i, T_j), Post(P_i, T_j), M_0, \chi \rangle$ *verifying the following conditions:*

- X_{DF} *is a finite set of continuous state variables,* $X_{DF} \subset \mathbb{R}$ *;*
- X_D *is a finite set of discrete state variables,* $X_D \subset \mathbb{Z}^+$ *;*
- T_D *is a finite set of discrete transitions ;*
- T_{DF} *is a finite set of differential transitions ;*
- P_D *is a finite set of discrete places ;*
- P_{DF} *is a finite set of differential places ;*
- $Pre(P_i, T_j)$ *is a function that defines arcs from a place to a transition with* $Pre(P_i, T_j) \in \mathbb{R}$*;*
- $Post(P_i, T_j)$ *is a function that defines arcs from the transition with* $Post(P_i, T_j) \in \mathbb{R}$*;*
- $M_0 = [M_{C0}; M_{D0}]$ *is the initial marking of discrete and continuous states;*
- $\chi \subseteq (P_D \times T_D) \cup (T_D \times P_D)$ *is a set of arc which consist of a set of ordinary arcs and a set of inhibitor arcs;*
- $P \cap T = \emptyset$ *and* $P \cup T \neq \emptyset$

5. Modelling of supervisory control by DHPN

Once the design of operational modes is done, let us modelled by DHPN. Indeed, supervisory is led by this level which selects the operating mode and the coupling of the sources and load at the DC microgrid. Supervisory system is based on three inputs and three outputs as illustrated by Figure 3. According to inputs information,

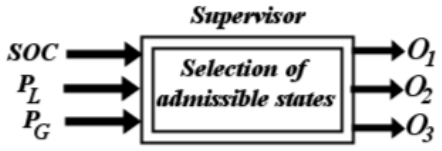

Figure 3: Supervisory system

essentially continuous events, supervisor assesses power balance of each source, then drives information to different outputs. Otherwise, it makes sure those informations achieve to desirable states.

Remark: It's important to note according to Figure 4, the firing of some transitions required to consider constraints mentioned in Table 1; in the case of structural conflicts, the priorities of firing the transitions can be presented. So, the priority of a transition will be fixed in simulation.

Technium Vol. 2, Issue 7 pp.64-76 (2020)
ISSN: 2668-778X
www.techniumscience.com

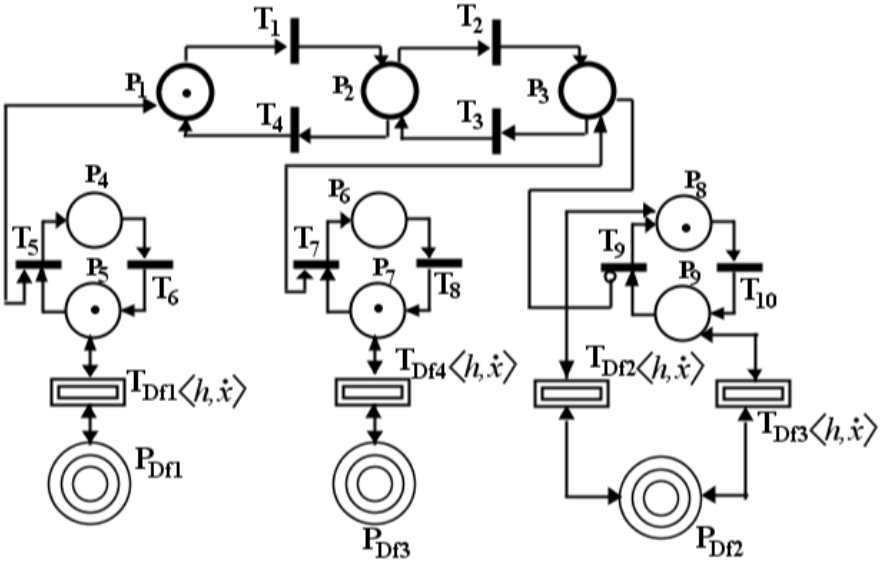

Figure 4: Differential Petri net model of High level control

Table 2: Legend of Figure 4

Continuous events		continuous states	
T_{Df1}	Calculation of P_{pv} and P_{hyd}	P_{Df1}	Power of PV and Power of $pico-hydroelectric$
T_{Df2}, T_{Df3}	Calculation of V_{bat}&SOC	P_{Df2}	Voltage battery and SOC
T_{Df4}	Calculation of P_{load}	P_{Df3}	Load power
Discrete events		Discrete states	
T_1	Switch from Mode I to MODE II	P_1	*MODE I*
T_2	Switch from Mode II to MODE III	P_2	*MODE II*
T_3	Switch from Mode II to MODE III	P_3	*MODE III*
T_4	Switch from Mode II to MODE I	P_4	*Plants and Batteries supply*
T_5	Coupled Plants and batteries	P_5	*Generators in stand alone mode*
T_6	Turn On stand alone mode	P_6	*Uncoupled load*
T_7	Switch OFF loads	P_7	*Coupled load*
T_8	Switch ON loads	P_8	*Battery empty*
T_9	Run to discharge state	P_9	*Battery full*
T_{10}	Run to charge state	h	the simulation step

6. Simulations and results

Assessment of the model was realised in the virtual environment MATLAB, composed of different subsystems, profile of loads presented in Figure 6 (b) see ([22]). Then depending on the power required and the type of our installation, we opte for the installation of two $5kwp$ power PV generators. It is made up of photovoltaic panels of type KD180GX-LP of SUD CONCEPT brand KYOCER, the energy storage system of a set of batteries. For each battery: stationary type, $V_n = 12V_{cc}$, $C_{rated} = 140Ah$. The BB has $V_T = 24Vcc$ and $C_T = 1400Ah$. The small hydraulic plant consists of an

Technium Vol. 2, Issue 7 pp.64-76 (2020)
ISSN: 2668-778X
www.techniumscience.com

asynchronous generator whose parameters are: $4kw$ and 1500 rpm Weather data for the location, for a typical weather year was taken from Cameroon Civil Aviation Authority located in the North region of Cameroon. Figure 5(a and b) shows temperature and hourly global horizontal radiation (W/m^2) of three days in different months (January, June and September) respectively of the chosen site. The flow profile used is illustrated by Figure 5(c).

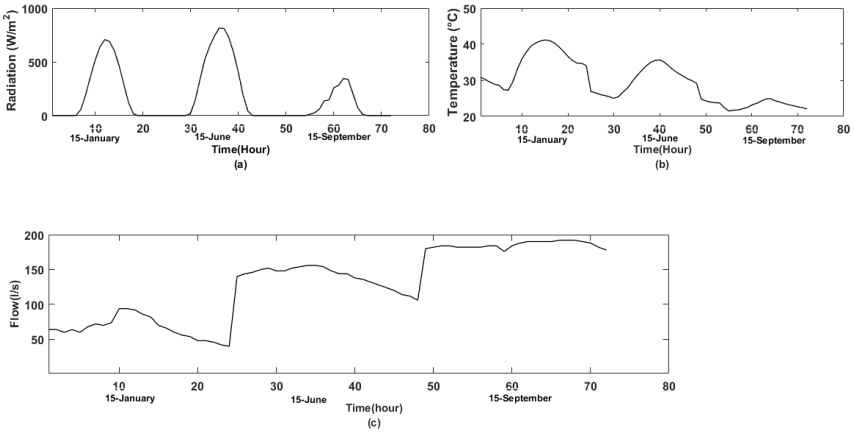

Figure 5: (a) Hourly global horizontal radiation; (b) Hourly temperature; (c) Exploited flow

DHPN model has the following initial marking : $M_0(t) = \begin{bmatrix} M_{D0} & M_{C0} \end{bmatrix}^T$,where $M_{D0} = \begin{bmatrix} 1 & 0 & 0 & 1 & 0 & 0 & 1 & 1 & 0 \end{bmatrix}^T$ and $M_{C0} = \begin{bmatrix} P_{GO} & P_{LO} & v_{bat0} & SCO_0 & i_{bat0} \end{bmatrix}^T = \begin{bmatrix} 2220 & 2295.9 & 182.20 & 0.50 & 0 \end{bmatrix}^T$

$P_{GO} = P_{php0} + P_{pv0}$. We obtained the following results for the continuous states:

Figure 6 represents the behaviour of the load and plants power without any supervisory system, and Figure 7 the behaviour of the system with supervisory system.

Furthermore, during the running of the model, many discrete markings are generated. Among we have a marking of each mode represented by :

$M_{D1} = \begin{bmatrix} 0 & 1 & 0 & 0 & 0 & 0 & 1 & 0 & 0 \end{bmatrix}^T$;

$M_{D2} = \begin{bmatrix} 0 & 0 & 1 & 0 & 1 & 0 & 1 & 0 & 1 \end{bmatrix}^T$;

$M_{D3} = \begin{bmatrix} 0 & 1 & 0 & 0 & 0 & 0 & 1 & 0 & 0 \end{bmatrix}^T$; and

$M_{D4} = \begin{bmatrix} 1 & 0 & 0 & 0 & 0 & 0 & 1 & 0 & 0 \end{bmatrix}^T$

The curves obtained in Figure 7 show the continuous behaviours for three days of operational system. Initially between $t = 1$ to $t = 16h$, the system is in MODE I. This implies that the generators are in stand alone mode, the battery bank is charged and the consumers are connected. In this case, tokens are in different places as mentioned in Figure 4; hence M_{D0}. After system runs to MODE II through place P_2 by firing T_1 between $t > 16h$ to $t < 33h$. In fact, during this mode, as show in Figure 7 (a), we observe that the load is fed by power produces by the generators and the energy

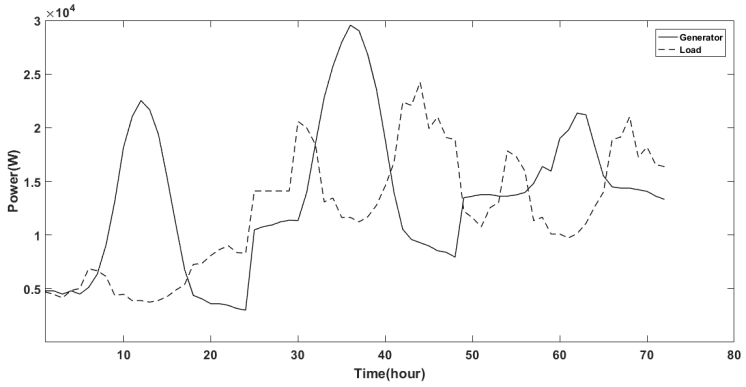

Figure 6: Power curves without supervision

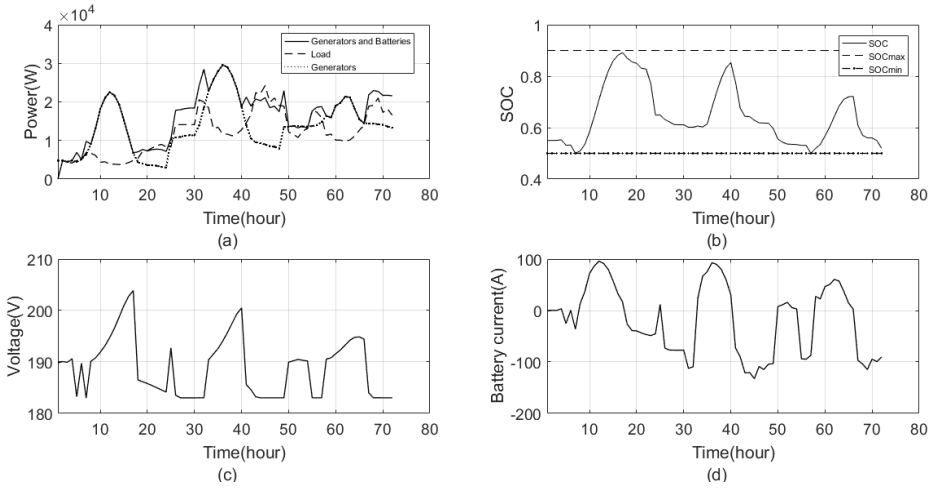

Figure 7: (a) Power ; (b) SOC; (c) battery voltage ; (d) battery current

in battery which is decreasing as illustrated to Figure 7(b). Furthermore, in $t > 33h$ to $t < 40h$ energy provided by the both generators is enough to satisfy the consumers, the progress of the system goes to place P_3 where we obtain M_{D2} by validating T_2 and T_6. In this phase, battery is recharged by the excess energy produces by the generators. After, between $t > 40h$ to $t < 48h$, the system returns to MODE II by firing T_4 we get M_{D3}, then M_{D4} by firing T_5, T_8 and T_9 at last return to initial state. . The progress of this operational system can be illustrated by the marking graph given by the Figure 8.

With $s_1 = \{T_1\}$; $s_2 = \{T_2, T_6\}$;$s_3 = \{T_3\}$;$s_4 = \{T_4\}$; $s_5 = \{T_5, T_8, T_9\}$ and $s_6 = \{T_1\}$.

Moreover, to evaluate power system reliability supervised, the criteria Loss of Power Supply Probability given by Equation 22

$$LPSP = \frac{\sum_{t=1}^{T} (P_c(t) + P_{bat}(t))}{\sum_{t=1}^{T} P_L(t)} \tag{22}$$

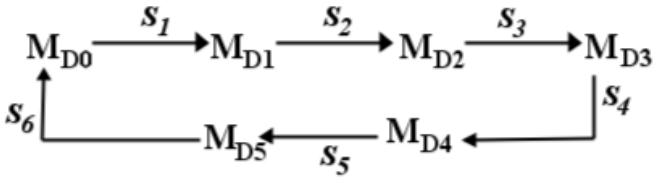

Figure 8: Marking graph

is used. It corresponds to the ratio of all energy deficit to the load demand during operational modes [23]. So according to the number of batteries, Table 3 presents different performances of the HRES.

Table 3: Performance criteria

Num bat	60	80	100
LPSP	0,0192	0,0102	0,00004

It follow that to ensure a better supply of the electrical energy of the load, we need 100 numbers of batteries, due to his low value of $LPSP$ which equal to 0.00004

7. Conclusion

This work is focused on the design of the supervisory control system by using Differential Hybrid Petri Net of a HRE system. We introduce a topology of our hybrid system with mathematical models of each considered component. Then, we described operational modes which are based on the level of energy in the storage system and ratio of available energy, moreover, for a better satisfaction of the consumers we evaluate the ability of the system to supply the load through $LPSP$. Eventually, results obtained show the relevance of the proposed management methodology. Future works continue investigation in order to compare our approach to others methods, and to develop optimal control with Model Predictive Control technique.

References

[1] Kyriakarakos G, Dounis A I, Arvanitis K G and Papadakis G 2017 *Applied Energy* **187** 575 – 584 ISSN 0306-2619
[2] Diaf S, Diaf D, Belhamel M, Haddadi M and Louche A 2007 *Energy Policy* **35** 5708 – 5718 ISSN 0301-4215
[3] Khelif A, Talha A, Belhamel M and Arab A H 2012 *International Journal of Electrical Power and Energy Systems* **43** 546 – 553 ISSN 0142-0615
[4] Nfah E and Ngundam J 2009 *Renewable Energy* **34** 1445 – 1450 ISSN 0960-1481
[5] Kenfack J, Neirac F P, Tatietse T T, Mayer D, Fogue M and Lejeune A 2009 *Renewable Energy* **34** 2259 – 2263 ISSN 0960-1481

[6] Abanda F 2012 *Renewable and Sustainable Energy Reviews* **16** 4557 – 4562 ISSN 1364-0321
[7] Lu D, Fakham H, Zhou T and Franois B 2010 *Renewable Energy* **35** 1117 – 1124 ISSN 0960-1481
[8] Nfah E, Ngundam J, Vandenbergh M and Schmid J 2008 *Renewable Energy* **33** 1064 – 1072 ISSN 0960-1481
[9] Badoud A, Khemliche M, Bacha S and Raison B 2013 *2013 International Renewable and Sustainable Energy Conference (IRSEC)* pp 298–303
[10] Tafticht T, Atif K and Agbossod K 2003 *IEEE CCECE* **1 (4-7)** 543–546
[11] Giua A and DiCesare F 1994 *IEEE Transactions on Robotics and Automation* **10** 185–195 ISSN 1042-296X
[12] Murata T 1989 *Proceedings of the IEEE* **77** 541–580 ISSN 0018-9219
[13] Khawaja Y, Allahham A, Giaouris D, Patsios C, Walker S and Qiqieh I 2019 *Applied Energy* **250** 257 – 272 ISSN 0306-2619
[14] Javaid C J, Allahham A, Giaouris D, Blake S and Taylor P 2019 *The Journal of Engineering* **2019** 3918–3922
[15] Sousa J R B and Lima A M N 2008 *2008 IEEE International Symposium on Industrial Electronics* pp 1861–1866 ISSN 2163-5137
[16] David A, Joseph E, Ngwa N and Arreyndip N 2018 *International Journal of Renewable Energy Research* **8** 649–660
[17] Paruchuri V K, Davari A and Feliachi A 2005 *Proceedings of the Thirty-Seventh Southeastern Symposium on System Theory, 2005. SSST '05.* pp 221–224 ISSN 0094-2898
[18] Molua E and M-Lambi C 2006 *CEEPA, Pretoria*
[19] Benmessaoud M, Zerhouni F, Zegrar M, Stambouli A B and Tioursi M 2010 *Computers and Mathematics with Applications* **60** 1124 – 1134 ISSN 0898-1221 pCO 2010
[20] Valenciaga F, Puleston P F, Battaiotto P E and Mantz R J 2000 *IEE Proceedings - Control Theory and Applications* **147** 680–686 ISSN 1350-2379
[21] Demongodin I and Koussoulas N T 2006 *IEEE Transactions on Systems, Man, and Cybernetics, Part C (Applications and Reviews)* **36** 543–553 ISSN 1094-6977
[22] Nfah E, Ngundam J and Tchinda R 2007 *Renewable Energy* **32** 832 – 844 ISSN 0960-1481
[23] Javed M S, Song A and Ma T 2019 *Energy* **176** 704 – 717 ISSN 0360-5442